

## Experimental investigation on the stability behavior of a natural circulation system: from single-phase to two-phase and from low to high inventory condition

M. R. Gartia

Reactor Engineering Division  
Bhabha Atomic Research Centre, Trombay  
Mumbai-400 085  
mrgartia@barc.gov.in

P. K. Vijayan

Reactor Engineering Division  
Bhabha Atomic Research Centre, Trombay  
Mumbai-400 085  
vijayanp@barc.gov.in

A.K. Nayak

Reactor Engineering Division  
Bhabha Atomic Research Centre, Trombay  
Mumbai-400 085  
arunths@barc.gov.in

D. Saha

Reactor Engineering Division  
Bhabha Atomic Research Centre, Trombay  
Mumbai-400 085  
dsaha@barc.gov.in

### Abstract

The flow instability behaviour of a boiling two-phase natural circulation loop was studied at reduced inventory conditions, which is important during a LOCA situation in a nuclear reactor with non-availability of circulating pumps. For this, experiments were conducted at low steam drum levels. Large amplitude U-tube type oscillations were observed at low power condition when the system was mostly under single-phase condition. With rise in power when boiling was initiated in the loop, low quality Type I density-wave instabilities were observed. The characteristics of Type I instabilities are found to be quite different from the oscillations observed under single-phase conditions. With further rise in power, the Type I instabilities were found to be suppressed. To understand the instability behaviour of the loop, stability maps were predicted using the computer code TINFLO-S under different pressure, power and steam drum level conditions and the predicted results were compared with the measured value.

### 1. Introduction

Boiling two-phase natural circulation loops have several applications in nuclear and process industries due to their simplicity, low maintenance and operational cost, etc. Many of the new generation reactors including that of the Indian Advanced Heavy Water Reactor (AHWR) (Sinha and Kakodkar (2006)) also rely on natural circulation for removal of fission heat generated in the reactor core. Currently operating PHWRs and PWRs depend on natural circulation for removal of core decay heat following non-availability of circulating pumps. In these reactors, in addition to

single-phase natural circulation, two-phase natural circulation can also occur if there is progressive decrease of system inventory following a LOCA situation. With decrease in system inventory, the pressure in the system also falls gradually and the decay power also reduces with time. Hence, it is important to study the natural circulation behaviour in such systems at reduced inventory conditions at different pressure and power levels.

One of the major characteristics of natural circulation is that it can be unstable depending on the system geometry and operating conditions. Flow instabilities are undesirable since they not only reduce the thermal margin but also make the system operation difficult. The characteristics of instabilities at different operating conditions can also be different. A literature review suggests several investigations have been carried out in the past to understand natural circulation instability behaviour in single and two-phase systems. Experimental investigations in two-phase natural circulation loops having single heated channel have been carried out by Jain et al. (1966), Chexal et al. (1973), Lee et al. (1990), Jiang et al. (1995) and Wu et al. (1996). They observed density wave instability in their experiments, which was found to be affected by channel exit restriction, inlet subcooling, pressure and channel inlet restriction. The effect of downcomer level was experimentally studied by Chexal et al. At low powers and low pressures, the natural circulation loops are susceptible to several types of instabilities as described in the literature by Boure et al. (1973), Lee and Ishii (1990), Aritomi et al. (1992), Kyung and Lee (1994), Jiang et al. (1995), Kyung and Lee (1996) and Nayak et al. (2006). Flashing, geysering and Type I density wave oscillations are typical examples. These instabilities may or may not occur in isolation.

In the present work, experiments have been carried out to understand flow instability behaviour of a boiling natural circulation loop at reduced inventory conditions. The experiments were carried out over a wide range of power and pressure conditions and from single-phase to two-phase conditions. The instability characteristics under single-phase condition were found to be quite different from that with initiation of boiling. Stability maps were predicted using the computer code TINFLO-S and the results were compared with the measured values.

## 2. Experimental set-up

A schematic of the experimental set-up is shown in Fig. 1. The experimental loop consists of a vertical tubular heater directly heated by electric current up to a maximum power of 80 kW. The inner diameter of heated section is 52.5 mm. Subcooled water enters the heater at the bottom and gets heated as it rises through the test section due to buoyancy. The steam water mixture coming out of the heater rises through the riser section and is passed on to a vertical separator. In the separator, the steam gets separated from the water by gravity. The steam then goes to the condenser where it gets condensed and the condensate falls back to the separator through a pipe that joins the separator at the bottom. The condenser is a 1-2 shell and tube type heat exchanger with steam condensing on the shell side and cooling water flowing in the tube side. The elevation of the primary loop is about 3.35 m and the length of the heated section (test section) is about 1.18 m. The horizontal length of the loop is 3.4 m. Further details of the experimental set up are given in the report by Kumar et al. (2000).

The natural circulation flow rate in the loop is measured by calibrating the pressure drop across 2 m length of horizontal pipe (the flow in this stretch of pipe is single-phase) under forced flow with a differential pressure transmitter. The pressure drop measured across this pipe is used to calculate the flow rate using the pipe friction factor correlation developed using the data from the calibration runs as shown in Fig. 2. This method is adopted to minimize the pressure losses in the loop (with the possible insertion of orifice or venturimeter), which has significant influence on the natural circulation behavior. The loop pressure is measured with a strain gauge type pressure transducer having sensitivity of 2.0 mV/V. Temperature at various locations are measured with K-type (Chromel-Alumel), 1 mm OD mineral insulated thermocouples. All the data were recorded on-line using a fast data acquisition system. The sampling time was one second.

Accuracy of measurement are as follows:

Temperature:  $\pm 0.75\%$  of span (0-400 °C)

Pressure :  $\pm 0.35\%$  of span (100 bar)

Level :  $\pm 0.2\%$

The experimental conditions and loop dimensions are shown in Table 1.

Table 1: Experimental conditions and geometry of the loop

|               |                              |             |
|---------------|------------------------------|-------------|
| Pressure      | 1 bar to 10 bar              |             |
| Working fluid | Water                        |             |
| Power         | 0 to 70 kW                   |             |
| Level         | 5 % to 85 % of full SD level |             |
| Component     | Pipe                         | I.D (in mm) |
| Test Section  | 50 mm NB Sch. 40             | 52.5        |
| Loop          | 50 mm NB Sch. 80             | 49.25       |
| Steam Drum    | 150 mm NB Sch. 120           | 139.7       |

## 3. Experimental procedure

The primary loop was filled with water under ambient conditions and all instruments were vented. The loop was pressurized to required initial pressure by using nitrogen and then the steam drum (SD) level was brought to required level by draining the inventory. Then experiments were carried out by supplying power to the test section. Power was raised in steps of 2 kW in every 30 minutes when the natural circulation flow reached a steady state. To maintain the required pressure after power is raised, venting of nitrogen from SD was carried out. This was continued till temperature readings at the entry of the steam drum and at the condenser are equal and corresponds to the saturation temperature of prevailing SD pressure to ensure complete evacuation of nitrogen from the system. If the pressure still increases with the increase in power, pressure was stabilized by adjusting the condenser cooling water flow rate.

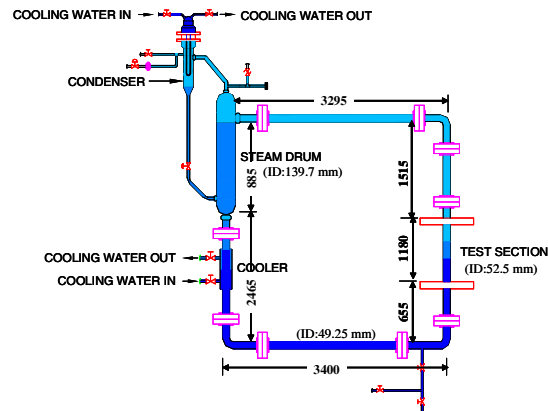


Fig. 1: Schematic of High Pressure Natural Circulation Loop

## 4. Analytical tool

For analyzing the natural circulation behaviour of the loop, the computer code TINFLO-S (Nayak et al. (1998)) was used. The formulation of the code is based on one dimensional, homogeneous two-phase flow model. The details about the mathematical formulation are given in the reference (Nayak et al. (1998)).

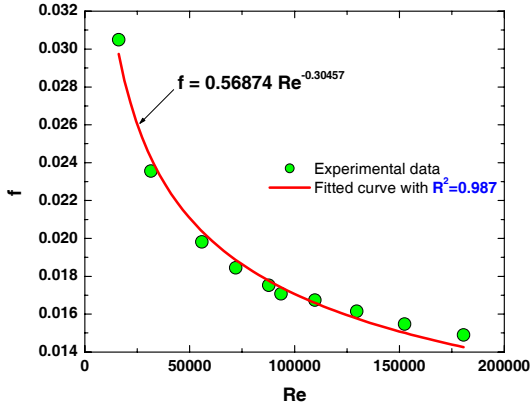


Fig. 2: Calibration curve for the friction factor in HPNCL

## 5. Results and Discussions

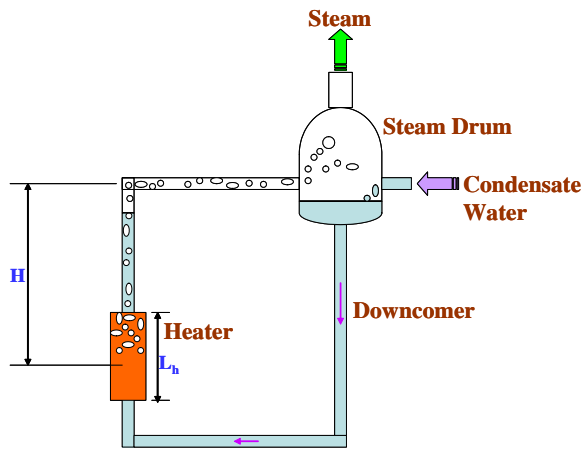


Fig. 3: Schematic of HPNCL under low SD level condition

A schematic of low steam drum level situation in high pressure natural circulation loop is shown in Fig. 3. Because of low steam drum level, a U-tube manometer type situation arises in the natural circulation system since the loop is not completely filled with the circulating fluid.

### 5.1 Single-phase natural circulation

Initially, the loop was filled with water at room temperature and pressurized to the required pressure (2 bar) with the help of nitrogen. The initial fluid temperature was atmospheric. When the power supply was turned on, the fluid in the vicinity of the heater

becomes lighter due to heat addition and rises upward due to buoyancy. To fill the void thus created the heavier denser fluid from the downcomer moves into the test section. This gives rise to a local flow in the loop (the gross flow is zero). However, the resistive frictional and inertia forces try to bring back the fluid to its original position. This results into flow reversals in the loop as observed in the figure 4. The flow never reaches a stable state in this case. Then the power was increased to 10 kW from the above case of 4 kW and the pressure was maintained constant at 2 bar. The fluid temperature at heater outlet is found to reach closer to saturation temperature as observed in Fig. 5 even though no boiling occurs in the loop. The flow was found to be oscillatory with irregular flow reversals. However, the amplitude of oscillation was found to be much larger than that observed at low power. The frequency of large amplitude oscillation was found to be almost periodic in both cases. The frequency of this oscillation was found to be larger at low power than at high power.

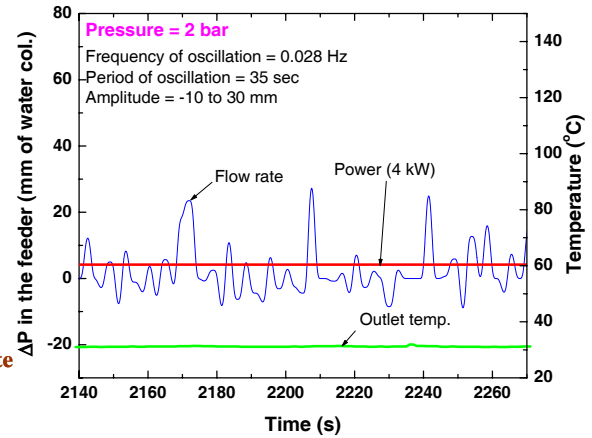


Fig. 4: Typical flow instability behaviour at low power under single-phase condition (power 4 kW)

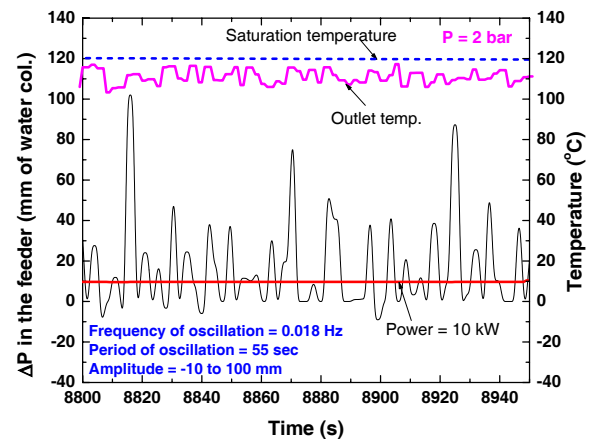


Fig. 5: Typical flow instability behaviour at low power under single-phase condition (power 10 kW)

## 5.2 Two-phase natural circulation

Subsequently, the power was raised to 12 kW at which the fluid temperature at heater outlet was found to be almost the same as the corresponding saturation temperature at 2 bar pressure (Fig. 6). Hence, boiling is initiated in the fluid at this operating condition. Unlike in the single-phase condition, the flow was found not to reverse with initiation of boiling. The characteristics of oscillation were similar as previous cases (i.e. periodic large amplitude oscillation with few small amplitude oscillations in between) even though there is no flow reversals. However, flow stagnation occurs periodically which is a safety concern in nuclear reactors. The amplitude of oscillation was found to be larger than under single-phase condition. The frequency of large amplitude oscillation was also found to increase with initiation of boiling in the loop.

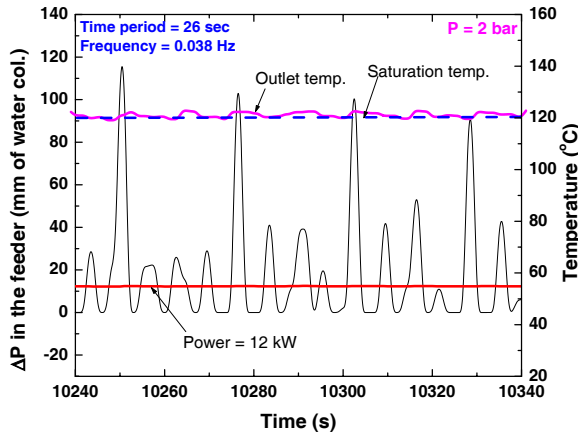


Fig. 6: Typical flow instability behaviour at low power under two-phase condition (initiation of boiling, power 12 kW)

With further rise in power to 14 kW, the flow oscillations were found to be more regular or periodic as observed in Fig. 7. Like the previous cases, the frequency and amplitude of oscillations were found to increase with increase in power. However, if the power is further increased, the flow oscillations are found to be damped as seen in Fig. 8. These oscillations are the so-called Type I density-wave instability (Fukuda and Kobori (1979)). Normally, these instabilities occur in natural circulation loops with tall riser. At low flow quality condition, the buoyancy force can fluctuate a lot even with a small fluctuation in quality due to larger variation of void fraction with quality. With increase in power, the flow quality increases and the variation of voids fraction with quality reduces. As a result, the Type I instability dies down with rise in power.

## 5.3 Effect of pressure on two-phase natural circulation

To understand the effect of pressure on natural circulation instability, experiments were conducted at higher pressures and the same heater power conditions.

Fig. 9 shows the results obtained at the heater power of 14 kW at a pressure of 5 bar. The amplitude of oscillations with initiation of boiling in the loop, is found to be lower than the corresponding results shown in Fig. 7. With further rise in power to 16 kW, the amplitude of oscillations is found to reduce like that at low pressure condition (2 bar). The time period of oscillation was found to be closer to that observed at 2 bar pressure.

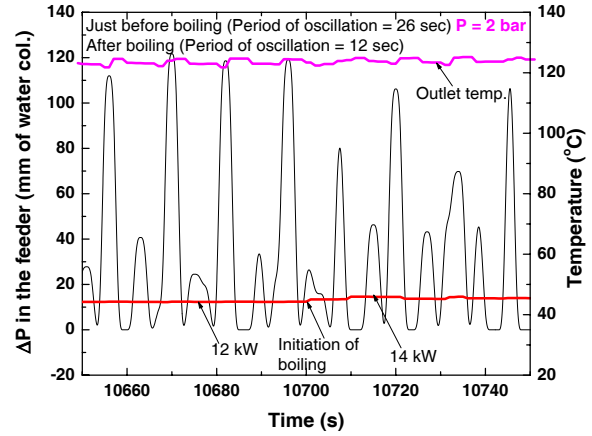


Fig. 7: Typical flow instability behaviour at low power under two-phase condition (power 14 kW)

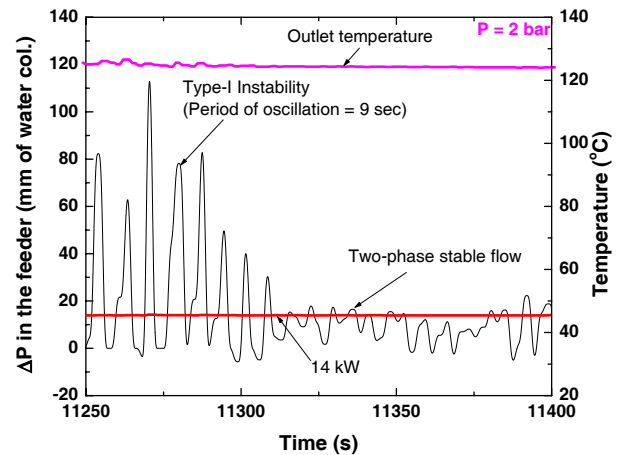


Fig. 8: Suppression of Type I instability with rise in power.

With further rise in pressure to 30 bar, the oscillations observed in single-phase natural circulation was found to be more regular (Fig. 10) than that observed at 2 bar (Fig. 5). The amplitude of oscillation was found to be much lower than that observed at 2 bar. Similar

behaviour is observed under two-phase natural circulation conditions at higher power (26 kW) at this pressure (Fig. 11).

#### 5.4 Stability map for the loop

It is of interest to investigate the effects of various operating conditions on the flow stability of this loop. The main parameters which affect the flow stability are: pressure, power and steam drum level for a given subcooling. Using the computer code TINFLO-S (Nayak et al. 1998), the flow stability behaviour of the loop has been predicted. The effect of pressure, power and steam drum level on the stability as predicted by the code, is shown by the 3-dimensional stability map in Fig. 12. It is observed that with increase in steam drum level, the threshold power for stability initially increases. This show that higher steams drum level stabilizes the natural circulation.

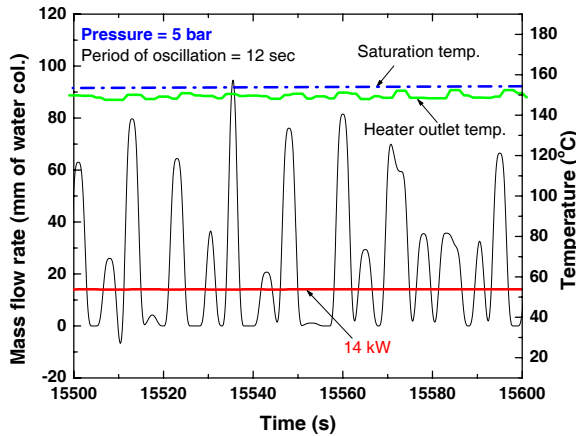


Fig. 9: Effect of pressure on flow instability behaviour at low power under two-phase condition (power 14 kW)

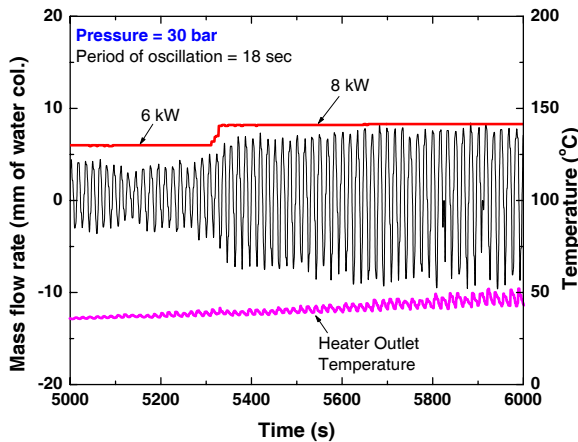


Fig. 10: Effect of power and pressure on flow instability behaviour at low power under single-phase condition.

With increase in power, the flow stabilizes due to damping of Type I instability as observed in the experiments. Similar behaviour is also observed for the effect of pressure on stability. Figure 13 shows a comparison of the threshold of instability between the code predictions and the measured data. It can be seen that some of the measured stable data points lie in the predicted unstable region. This is because the homogeneous model that is used for stability analysis, predicts a more conservative stability map (Nayak et al. 2006).

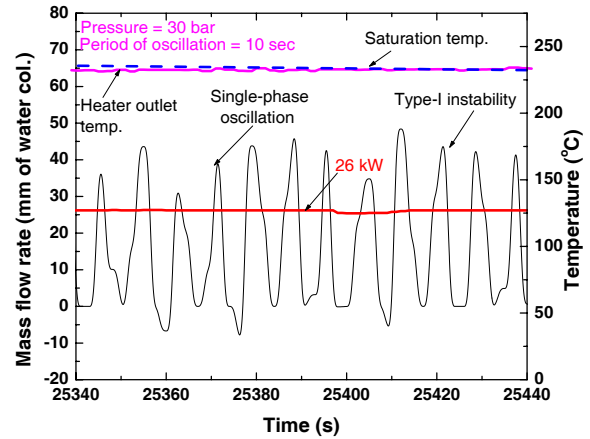


Fig. 11: Effect of pressure on flow instability behaviour at high power under two-phase condition (power 28 kW)

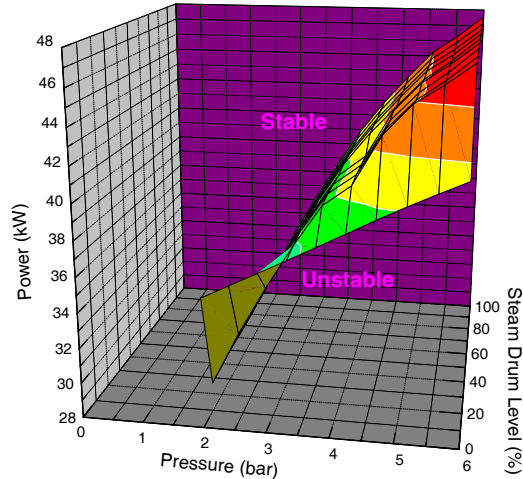


Fig. 12: Predicted stability map for HPNCL

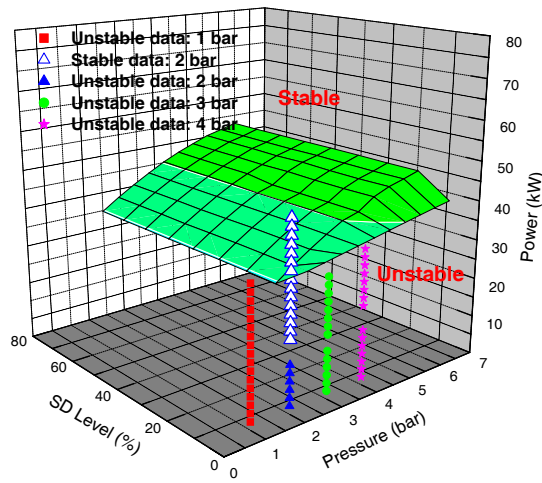


Fig. 13: Comparison of predicted stability behaviour of the loop and the measured data.

## 6. Conclusions

The flow instability behavior of a closed natural circulation loop was studied both experimentally and analytically. The experiments were conducted at low steam drum levels due to its importance for the heat removal rate in nuclear reactors in a LOCA situation with non-availability of circulating pumps. The conclusions can be drawn as follows:

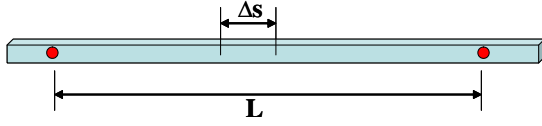
- At low heater power under single-phase condition flow reversal with irregular flow oscillations were observed.
- The periodic large amplitude oscillation observed under low power conditions gradually damp out with inception of boiling due to increase in heater power.
- The frequency of high amplitude oscillation was found to decrease with power under single-phase condition whereas with the inception of boiling the frequency of oscillation increased.
- The flow oscillation was found to be more regular with the increase in pressure. Also the amplitude of oscillation decreased with rise in pressure.
- The stability behavior of the loop was also compared with analytical results and found to be in good agreement.

## 7. References

1. Aritomi, M., Chiang, J.H., Nakahashi, T.M., Wataru, M. and Mori, M., "Fundamental study on thermo-hydraulics during start-up in a natural circulation Boiling Water Reactor (I) Thermohydraulic Instabilities", *Journal of Nuclear Science and Technology*, Vol. 29, pp. 631-640, 1992.
2. Boure, J.A., Bergles, A.E. and Tong, L.S., "Review of two-phase flow instability", *Nuclear Engineering and Design*, Vol. 25, pp. 165-192, 1973.
3. Chexal, V.K. and Bergles, A.E., "Two-phase flow instabilities in a low pressure natural circulation loop", *AIChE Symposium Series*, Vol. 69, pp. 37-45, 1973.
4. Fukuda, K. and Kobori, T., "Classification of two-phase flow instability by density wave oscillation model", *J. Nucl. Sci. Technology*, Vol. 16, pp. 95-103, 1979.
5. Jain, K.C., Petric, M, Miller, D. and Bankoff, S.G., "Self sustained hydrodynamic oscillations in a natural circulation boiling water loop", *Nuclear Engineering and Design*, Vol. 4, pp. 233-252, 1966.
6. Jiang, S.Y., Yao, M.S., Bo, J.H. and Wu, S.R., "Experimental simulation study on start-up of the 5 MW nuclear heating reactor", *Nuclear Engineering and Design*, Vol. 158, pp. 111-123, 1995.
7. Kumar, N., Rajalakshmi R., Kulkarni R. D., Sagar T. V., Vijayan P. K. and Saha D., "Experimental investigation in high pressure natural circulation loop", *BARC/2000/E/002*, February 2000.
8. Kyung, I.S. and Lee, S.Y., "Experimental observations in an open two-phase natural circulation loop", *Nuclear Engineering and Design*, Vol. 128, pp. 317-330, 1991.
9. Lee, S.Y. and Ishii, M., "Characteristics of two-phase natural circulation in Freon-113 boiling loop", *Nuclear Engineering and Design*, Vol. 121, pp. 69-81, 1990.
10. Nayak, A.K., Vijayan, P.K., Saha, D., Venkat Raj, V. and Aritomi, M., "Linear analysis of thermodynamic instabilities of the Advanced Heavy Water Reactor (AHWR)", *Journal of Nuclear Science and Technology*, Vol. 35, pp. 768-778, 1998.
11. Nayak, A.K., Dubey, P., Chavan, D.N. and Vijayan, P.K., "Study on the stability behavior of two-phase natural circulation systems using a four equation drift-flux model", *Nuclear Engineering and Design*, 2006 (to appear).
12. Sinha, R.K. and Kakodkar, A., Design and development of the AHWR-the Indian thorium fuelled innovative nuclear reactor, *Nuclear Engineering and Design*, 236, Issues 7-8, pp. 683-700, 2006.
13. Wu, C.Y, Wang, S.B. and Chin-Pan, "Chaotic oscillations in a low pressure two-phase natural circulation loop", *Nuclear Engineering and Design*, Vol. 162, pp. 223-232, 1996.

## APPENDIX

### Calculation of transient mass flow rate from pressure drop data



The differential momentum equation applicable for a segment of the loop can be written as

$$\frac{\partial}{\partial t}(\rho u) + \frac{\partial}{\partial s}(\rho u u) = -\frac{\partial p}{\partial s} - \rho g \sin \theta - \frac{f \rho u^2}{2D} - \frac{K \rho u^2}{2L}$$

For a horizontal pipe, buoyancy = 0 as  $\sin \theta = 0$

Incompressible flow,  $\frac{\partial u}{\partial s} = 0$  (from conservation of mass)

For an unrestricted pipe like the present horizontal section,  $K = 0$ . Therefore, the momentum equation becomes,

$$\frac{d}{dt}(\rho u) + = -\frac{\partial p}{\partial s} - \frac{f \rho u^2}{2D}$$

$$\frac{d}{dt} \left( \frac{W}{A} \right) = -\frac{\partial p}{\partial s} - \frac{f W^2}{2D \rho A^2}$$

Integrating

$$\frac{d}{dt} \left( \frac{W}{A} \right) \int ds = - \int \frac{\partial p}{\partial s} ds - \frac{f W^2}{2D \rho A^2} \int ds$$

$$\frac{L}{A} \frac{dW}{dt} = \Delta p(t) - \frac{f L W^2}{2D \rho A^2}$$

$$\frac{L}{A} \frac{W_{n+1} - W_n}{\Delta t} = \Delta p(t) - \frac{a}{(DW/A\mu)^b} \frac{LW^2}{2D\rho A^2}$$

$$\frac{L}{A} \frac{W_{n+1} - W_n}{\Delta t} = \Delta p(t) - \frac{a L W_{n+1}^{2-b} \mu^b}{2D^{1+b} \rho A^{2-b}}$$

where  $W_{n+1}$ : flow at current time step

$W_n$ : flow at previous time step

Calculation was proceed from the first non-zero value of  $\Delta p(t)$  for which  $W_n = 0$ .